LIME MORTAR AND PLASTER: A RADIOCARBON DATING TOOL FOR DATING NABATEAN STRUCTURES IN PETRA, JORDAN

Khaled Al-Bashaireh

Department of Archaeology, Yarmouk University, Postal code 211-63, Irbid, Jordan. Corresponding author. Email: khaledsm@email.arizona.edu.

Gregory W Hodgins

NSF Arizona Accelerator Mass Spectrometry Laboratory, Physics Building, 1118 East Fourth Street, PO Box 210081, University of Arizona, Tucson, Arizona 85721-0081, USA.

ABSTRACT. This research aims at radiocarbon dating 2 structures of archaeological interest from Petra, south Jordan, using lime plaster and mortar. Initially, the samples' content of calcareous contamination was examined by petrography and cathodoluminescence. In order to date clean lime binders, the samples were gently crushed and 63–45 μm powders were collected by dry sieving, then the CO_2 gases, collected by a hydrochloric acid hydrolysis of the powders, were dated. The interpreted ^{14}C dates clarify the chronology of the studied structures, show an agreement with the archaeological and historical data, and may indicate the efficiency of the cleaning and hydrolysis procedures.

INTRODUCTION

Archaeologists usually depend on archaeological materials, mainly pottery and written inscriptions, to date and build the chronology of the archaeological sites they are excavating. However, it is often difficult to find a suitable material whose age can reliably be assumed to represent the time of the construction of archaeological structures. In Petra, south Jordan (Figure 1), the date of the construction of several structures of historic interest cannot be confirmed by written sources and datable artifacts in primary contexts and/or a dendrochronological dating method. Nevertheless, these structures have sufficient quantities of the original lime mortar and lime plaster from the early stage of their construction. Gypsum- and lime-based mortar, plaster, and stucco were widely used in Petra (Zayadine 1987). They were used for constructing its free-standing structures, decorations, and covering the façades of its monuments and tombs carved in the cliffs of the mountains. Since there is a strong need to clarify the chronology of these structures, we are at present left with mortars and plasters as the only possibility for ^{14}C dating them. This material offers a potential dating key to the Nabateans' structures in Petra.

Plasters and mortars can be dated by optically stimulated luminescence (OSL) or thermoluminescence (TL) dating sand and pottery inclusions within them and radiocarbon dating of organic inclusions they contain and/or the lime binder itself after it has absorbed atmospheric carbon dioxide to form the plaster or mortar matrix. Several studies of dating mortars and plasters have focused on dating charcoal or organic inclusions. This approach has been used for dating structures at Petra (Al-Bashaireh and Hodgins 2011a). Most of these dates, derived from charcoals, woods, and straws teased out of plaster and mortar samples, were in concordance with the samples' historic data. However, ^{14}C dating organic inclusions does not always work. Tubbs and Kinder (1990) and Heinemeier et al. (2010) have warned about the unreliability of dating mortar based on organic inclusions because of the old-wood problem. The samples in their research produced dates older than expected. Moreover, many mortars and plasters do not contain organic inclusions, and alternative approaches are thus required. TL and OSL dating of sand aggregates from mortars and plasters, although theoretically possible, has not been reported in the literature.

Proceedings of the 6th International Radiocarbon and Archaeology Symposium, edited by E Boaretto and N R Rebollo Franco
RADIOCARBON, Vol 54, Nr 3–4, 2012, p 905–914

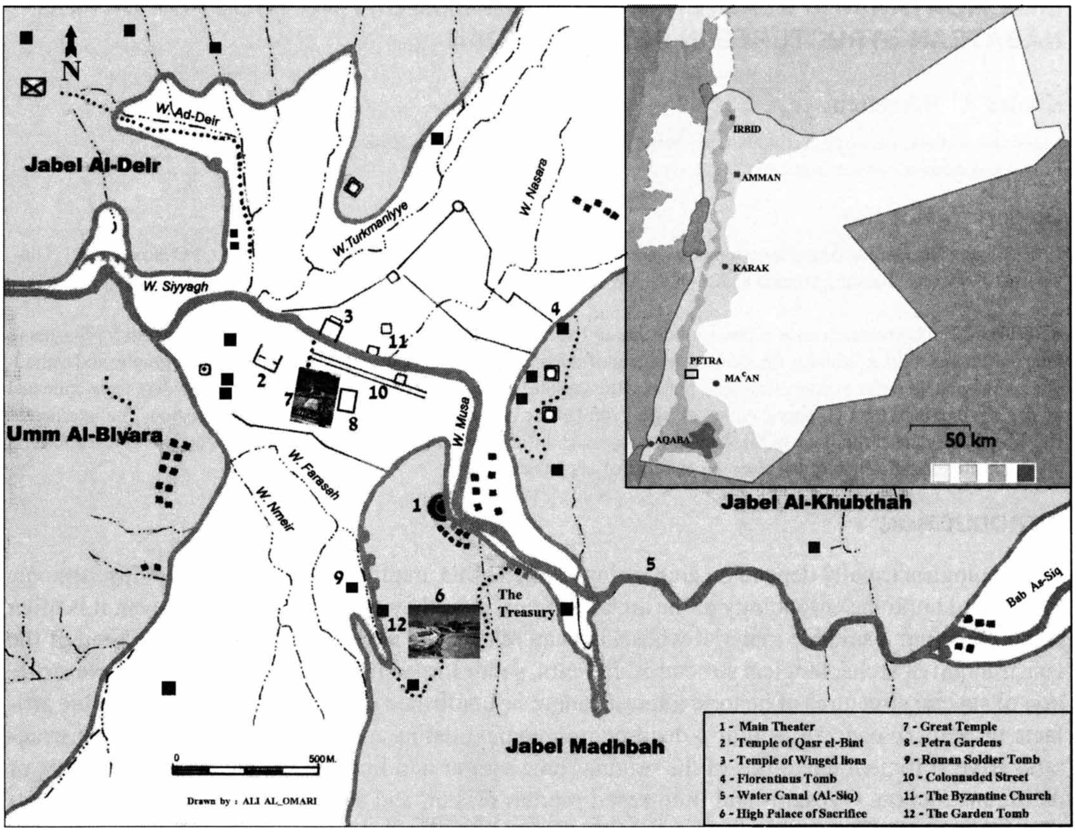

Figure 1 Location map (drawn by Ali Al-Omari)

Mortars and plasters that lack organic inclusions can, in some circumstances, be directly dated by the ^{14}C technique. In this work, we present 3 case studies of dating the lime binders of plaster and mortar samples lacking organic inclusions from 2 structures in Petra: the Great Temple and the High Place of Sacrifice. For details about Petra, its archaeology, geology, quarries, etc., see Al-Bashaireh (2008) and references therein.

The principle of ^{14}C dating lime mortars and plasters has been known since the 1960s (Labeyrie and Delibrias 1964; Stuiver and Smith 1965). When the mortar or plaster carbonate is homogeneous and free of contaminants, the method is straightforward. However, most often mortars and plasters contain carbonate contaminants that alter the ^{14}C content of the bulk sample. They are present as traces of incompletely burnt parent calcium carbonate left over from lime production, as inclusions introduced as part of the aggregate added to the slaked lime mix during the construction event, and as carbonate precipitates from groundwater infiltration and drying. The accurate ^{14}C dating of mortars and plasters is dependent upon the removal of these contaminants. Since the 1960s, development of the technique has focused on the strategies of sampling and physical and chemical pretreatments to identify and remove contaminants (e.g. Folk and Valastro 1976; Van Strydonck et al. 1986, 1992; Heinemeier et al. 1997, 2010; Sonninen and Jungner 2001; Hale et al. 2003; Lindroos 2005; Ringbom et al. 2006; Lindroos et al. 2007; Al-Bashaireh 2008). Modeling the dissolution of limestone-based mortar and postulating the criteria to interpret the ^{14}C ages were detailed by Lindroos et al. (2007), Al-Bashaireh (2008), and Heinemeier et al. (2010).

THE STRUCTURES

The Great Temple is one of the major archaeological and architectural elements of the Petra center. It is located south of the Temenos gate between Qasr el-Bint to the west and the Lower Market to the east and covers an area of about 7560 m^2 (see Figures 1 and 2a). The Great Temple is divided into 3 sections: the monumental entryway (the lower terrace or *propylaeum*); the lower Temenos (sacred lower terrace); and the upper Temenos and the Great Temple itself (the sacred enclosure) (Joukowsky 2005; Figure 2a). Considering Temple's architectural elements and pottery style, the excavators know its construction started during the 1st century BC; however, it was dramatically changed in later stages; these renovations have been variously placed sometime during the 1st century AD (Joukowsky 2002, 2007). The whole interior of the Temple was altered into a semicircular unroofed theater with tiers of seating for some 640 persons. The Temple collapsed during a major earthquake in AD 363 and was reused in Byzantine times (Joukowsky 2007).

A Roman-Byzantine bath complex was constructed within the Great Temple. It is located adjacent to the west boundary of the Upper Temenos and comprised bathrooms, *caldaria*, and a *frigidarium* (Figure 2b). The bath had been used for almost 500 yr, and underwent several stages of development. The fragments of 2 lamps found in the earliest deposits of the bath offered a *terminus post quem* date for the building of the baths in Phase VI (~1st century BC–1st century AD) of the Great Temple. This was around the time of the annexation of Nabataea by the Romans in AD 106 (Joukowsky 2007). A series of additions and alterations to the baths extended into Great Temple Phase VIII (about late 2nd century AD) and possibly even into Phase IX (bounded by the AD 363 earthquake). The added spaces include a small cistern, the bathroom and its anteroom, and a bench room or *apodyterium* (Figure 2b). The bathroom, the anteroom, and an elegant sink inside it would have highlighted the communal use of the bath complex (Joukowsky 2007).

The High Place of Sacrifice is located at the top of Al-Khubthah Mountain, which is ~3700 feet high. It can be reached by 2 narrow staircases; the first ascends from Wadi Farasah and the second from the south side of the outer Siq above the theater (Figure 1). At the High Place, there is an altar with a circular basin recessed in its center (Murray 1939). A water cistern, cut into the rock and lined with hard white plaster, is located nearby (see Figure 2c). The date of the High Place of Sacrifice is conjectural since there is no material evidence indicating when it was made. McKenzie (1990) dates its carving to the 1st century AD, while others date it to the period between 300 BC and AD 100 or to the time of the Edomites and suggest it was a place they might have worshiped (Robinson 1908).

MATERIALS AND METHODOLOGY

One white plaster (sample 1) and 1 light gray mortar (sample 2) were collected from the Great Temple, and 1 white plaster (sample 3) was collected from the High Place of Sacrifice (Figures 2a–c). Sample 1 was part of a remnant of plaster covering a column in the eastern triple colonnade built during Phase IV (~1st century BC–1st century AD) of the Great Temple construction (Joukowsky 2007). Sample 2 was from a light gray mortar layer bedding the anteroom at the Roman-Byzantine bath complex of the Great Temple. Sample 3 was collected from the upper level of plaster that lines a rock-cut water cistern located on the southern end of the recessed area of the High Place of Sacrifice. All of these sampling sites appeared original and undisturbed, and most probably represent remnants of the initial construction of the structures from which they were obtained. The plaster samples were collected from just under the original surface to try to eliminate dating anomalies seen in slow-hardening interior mortar joints (Van Strydonck et al. 1992). The few upper millimeters of surface were scraped away and then the samples carefully collected with a chisel. The bedding mortar sample was collected in a similar manner from an undisturbed area using a trowel and chisel.

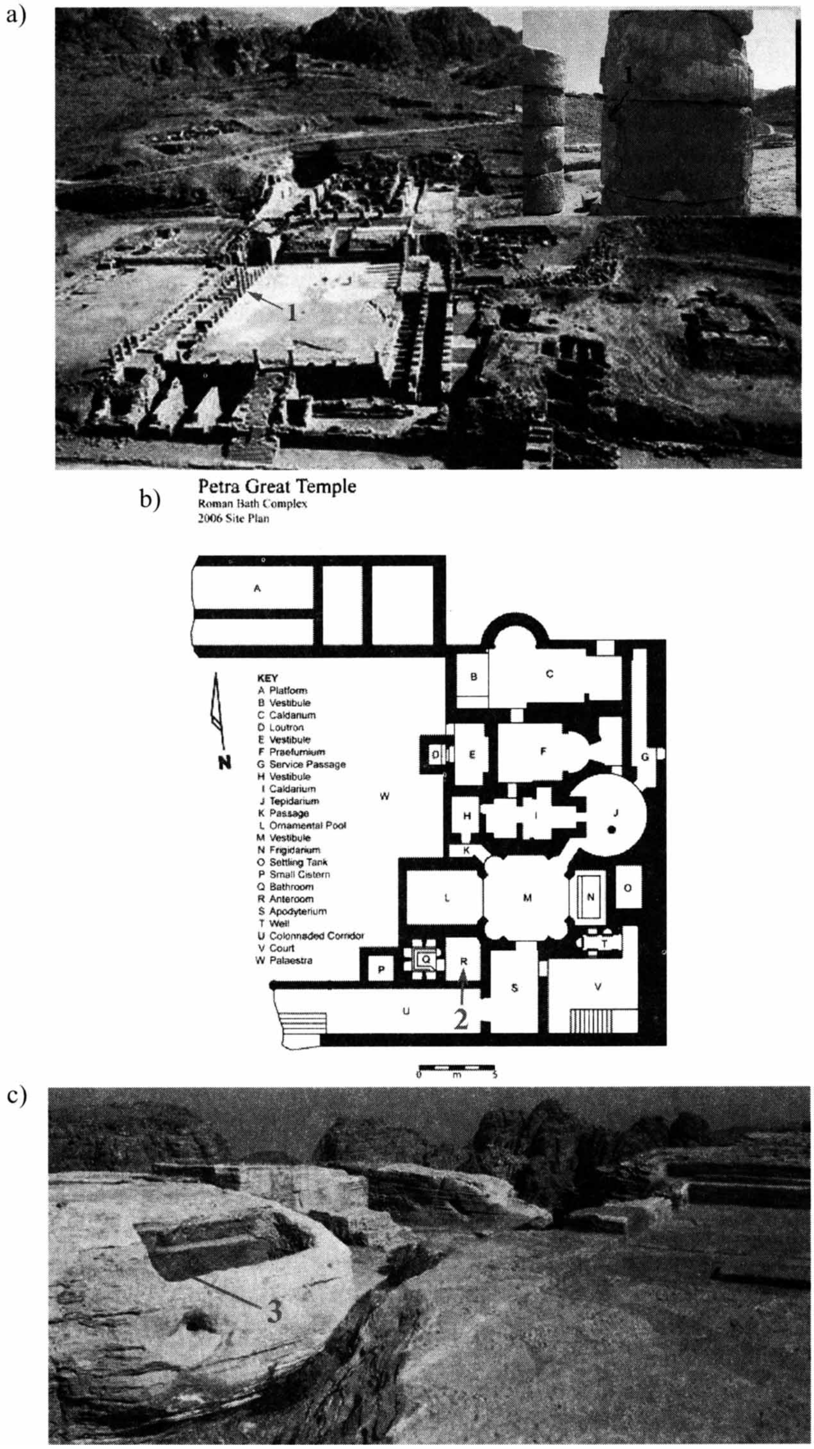

Figure 2 Locations of the samples: a) sample 1 from eastern colonnade at the Great Temple; b) sample 2 from the Roman-Byzantine bath complex of the Great Temple (modified after Joukowsky 2007); and c) sample 3 from water cistern at the High Place of Sacrifice.

Dating Lime Binder

The main task when dating the lime plaster is to collect a lime binder clean of old calcareous materials. Inclusions of carbonate minerals from aggregates or under-burned limestone, marble, shells, etc. produce spuriously old ages for the sample (Baxter and Walton 1970).

The mineral phase of the calcite of both the lime binder and the calcareous aggregates cannot be separated by a phase analysis using X-ray diffraction or chemical analysis. However, cathodoluminescence (CL), petrography, and scanning electron microscopy (SEM) are appropriate for their identification. In this study, a CL analysis was performed on polished surfaces of the 3 samples embedded in resin and on loose powders (63–45 μm) pretreated for hydrolysis. Thin sections of the 3 samples and a thin section of sample 3 stained with alizarin red were analyzed by polarized light microscopy. CL analyses examine the samples' content of contaminants from aggregates and incompletely burned limestone and aggregates of dolomite.

Sample preparation for ^{14}C dating involved gentle crushing, sieving to uniform grain size fractions, followed by an acid hydrolysis and collection of released carbon dioxide (see detailed discussion about these processes in Baxter and Walton 1970; Folk and Valastro 1976; Van Strydonck et al. 1986, 1989; Heinemeier et al. 1997). Samples 1 and 3 were prepared and dated twice to examine the reproducibility of the method.

In this work, 100–200 mg of 63–45 μm grain size powder was placed in a specially prepared hydrolysis vessel along with a magnet stirrer (Al-Bashaireh and Hodgins 2011b). The hydrolysis vessel incorporates an arm onto which a vacuum syringe was attached to allow a slow addition of 0.1M HCl. When a sufficient vacuum was reached (about 5×10^{-2} torr), aliquots of HCl were added to the powder, and the CO_2 gas evolved after each pulse of acid collected into a separate vessel. The amounts of HCl from the second aliquot onward were increased, while an excess of the HCl was added to the fifth aliquot to fully hydrolyze the remaining powder. The ^{14}C content of the 5 fractions was measured, and these results plotted versus the amount of the carbon collected from each, thus producing a profile of the ^{14}C age versus the extent of the hydrolysis for each sample, following the approach of Van Strydonck et al. (1986, 1989) and Heinemeier et al. (1997) (see below). The profiles were mainly interpreted following the criteria proposed by Lindroos et al. (2007) and Al-Bashaireh (2008) for HCl-hydrolyzed samples, and Heinemeier et al. (2010) in which lime powders were hydrolyzed with a diluted phosphoric acid. The conventional ^{14}C dates were calibrated using the OxCal v 3.10 program (Bronk Ramsey 1995, 2001) and the IntCal04 calibration curve data (Reimer et al. 2009).

RESULTS AND DISCUSSION

Petrographic analyses of the thin sections and CL analyses of polished surfaces of the resin-embedded samples showed contamination with limestone (see Figures 3a–c). Furthermore, the alizarin-stained thin section of sample 3 showed some dolomitic aggregates (Figure 3d). The CL analyses of the pretreated lime powders of 63–45 μm fraction, used for hydrolysis, showed a slight contamination with limestone, which might indicate the efficiency of the physical pretreatment.

The $\delta^{13}C$ values and the radiocarbon (BP) and the calibrated (cal BC/AD) ages of the samples are presented in Table 1, while the ^{14}C-F profiles are shown in Figures 4a–c, where the fraction (F) is the percentage of the weight of the carbon yield in mg of each CO_2 gas.

Sample 1, the column plaster from the eastern triple colonnade of the Great Temple: the $\delta^{13}C$ values show a sudden increase from the second fraction onward. Dating sample 1 was straightforward; the

https://doi.org/10.1017/S003382220004755X Published online by Cambridge University Press

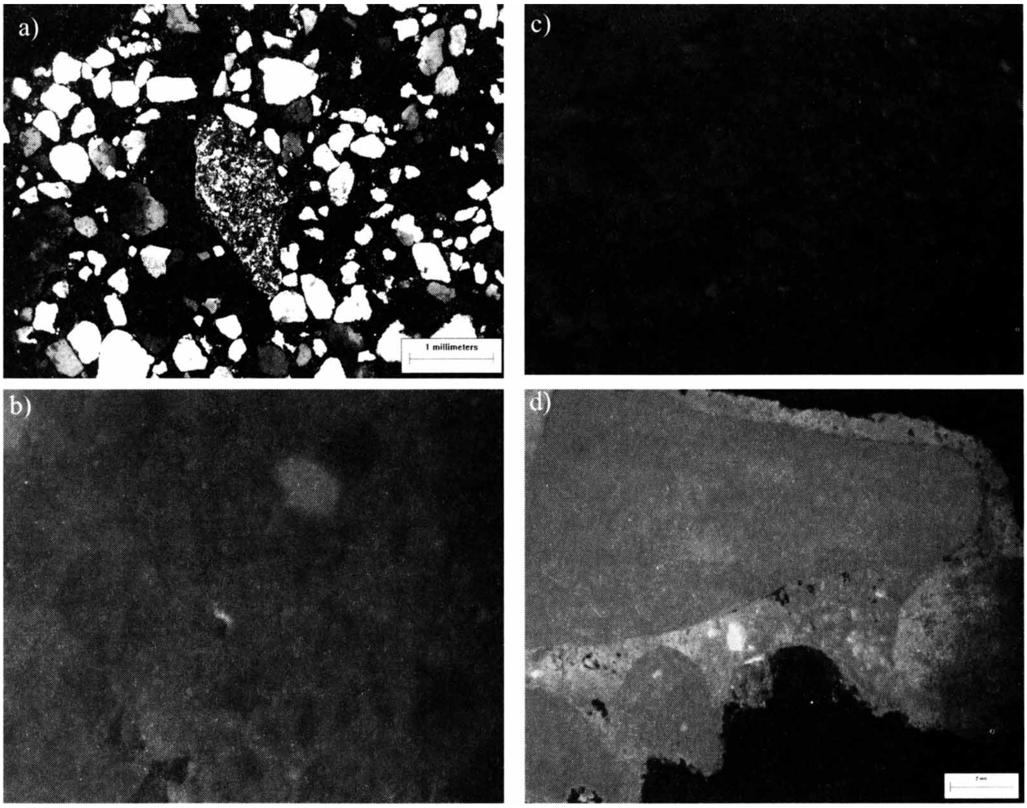

Figure 3 Petrographic and CL analyses: a) Thin-section photomicrograph of sample 1 shows a limestone grain surrounded by quartz grains; b) CL photomicrograph of sample 1 embedded in resin shows quartz grains in blue, limestone grains in orange, lime binder in tile red-black; c) CL photomicrograph of pretreated lime powders of 63–45 μm fraction of sample 1 shows some contaminants of red-orange limestone grains; d) stained thin-section photomicrograph of sample 3 shows the dark gray color of a rounded dolomite grain and the red color of limestone. (The online version of this article contains a full color version of the figure.)

date of the first fraction (1921 ± 34 BP, cal AD 1–210 at the 95% confidence interval, with 92% of the plot area falling between AD 1 and 140) most probably represents the date of the initial plastering of the column and, thus, the construction of the eastern colonnade. The date coincides with the Great Temple phases V (~1st century AD) and VI (AD 106 and 113/114 earthquake). The dates from the later hydrolysis fractions had progressively older ages, indicating either a calcareous sand was present in the aggregate, or the lime powder from which the plaster was made contained underburned limestone (Figure 5).

Measurement of a second preparation of sample 1 produced a similar hydrolysis profile, and date for the first fraction that duplicated the earlier result (1936 ± 56 BP, 47 cal BC–cal AD 220, 95% confidence interval) (see Figure 4a). Both of the profiles follow the third criterion of Al-Bashaireh (2008): the sample is slightly contaminated by an old carbon; therefore, they show an increase in the ages from the second fraction onward. The weighted average of the 2 dates (measured on the same object and representing the same event) produced a more precise date of the plastering of the column and most likely the construction date of the eastern colonnade (1925 ± 29 BP, cal AD 5–132, 95% confidence interval).

Table 1 Radiocarbon (BP) and calibrated (BC/AD) ages, ^{13}C values (‰) and the yield of carbon (mg). The bold rows are the weighted means of duplicate ^{14}C aged measurements

Lab code	Sample nr	^{14}C age (BP)	Calibrated age BC/AD (95.4%)	δ^{13}C (‰)	C (mg)	Material
AA78289	1a-1	1921 ± 34	AD 1–210	–15.4	0.59	Plaster
AA78290	1a-2	2186 ± 34		–9.4	0.62	Plaster
AA78291	1a-3	2355 ± 35		–9.2		Plaster
AA78291	1a-3	2379 ± 35		–9.2		Plaster
AA78292	1a-4	2404 ± 34		–9.4		Plaster
AA78292	1a-4	2341 ± 36		–9.4		Plaster
AA78293	1a-5	3103 ± 35		–9.1		Plaster
AA78293	1a-5	3097 ± 37		–9.1		Plaster
AA78289	1b-1	1936 ± 56	47 BC–AD 220	–10.9	0.7	Plaster
AA78290	1b-2	2008 ± 56		–12.3	0.7	Plaster
AA78291	1b-3	2003 ± 56		–12	0.65	Plaster
AA78292	1b-4	2295 ± 57		–9.4	1.72	Plaster
AA78293	1b-5	2348 ± 56		–9.2	5.8	Plaster
wtd mean	**1-1**	**1925 ± 29**	**AD 5–132**			**Plaster**
AA78322	2-1	1619 ± 36	AD 349–540	–10.8	0.55	Mortar
AA78323	2-2	1798 ± 44		–9.7	1.27	Mortar
AA78324	2-3	1849 ± 44		–10.5	2.45	Mortar
AA78325	2-4	2075 ± 36		–10.1	3.73	Mortar
AA78326	2-5	1908 ± 43		–10.6	4.84	Mortar
AA78083	3a-1	1961 ± 33	40 BC–AD 122	–8.8	0.64	Plaster
AA78084	3a-2	1901 ± 37		–17.2	0.53	Plaster
AA78085	3a-3	1990 ± 34		–10.5	0.78	Plaster
AA78086	3a-4	2312 ± 34		–4.1		Plaster
AA78086	3a-4	2334 ± 34		–4.1		Plaster
AA78087	3a-5	25,655 ± 34		–6.4	5.67	Plaster
AA78083	3b-1	1968 ± 56	157 BC–AD 138	–8.7	0.58	Plaster
AA78084	3b-2	1980 ± 56		–10.4	0.62	Plaster
AA78085	3b-3	2110 ± 57		–8.0	0.74	Plaster
AA78086	3b-4	2214 ± 57		–6.0	1.89	Plaster
AA78087	3b-5	2366 ± 56		–7.1	6.09	Plaster
wtd mean	**3-1**	**1962 ± 28**	**40 BC – AD 120**			**Plaster**

Sample 2, the Roman-Byzantine bath complex of the Great Temple: the most probable age of the sample is the date of the first fraction (1619 ± 36 BP, cal AD 349–540 at 95%, with 92.3% of the probability falling between AD 380–540); see the ^{14}C-F profile in Figure 4, Table 1, and Al-Bashaireh (2008:285–6: criteria 2). The ^{14}C-F profile shows an increase in the ages from the second fraction onward, indicating contaminations with the old carbon from calcareous added aggregates or under-burned limestone (Figure 4b). The diagram does not show any kind of plateau after the first or the second age, the sample is not hydraulic, and the δ^{13}C value of the first fraction is not very low but similar to the values of the other fractions. Therefore, these factors do not indicate reprecipitation of carbonates (see Lindroos et al. 2007; Al-Bashaireh 2008:284–6: criterion 2). The date strongly suggests that the bathroom and its anteroom were added during the Byzantine period. The

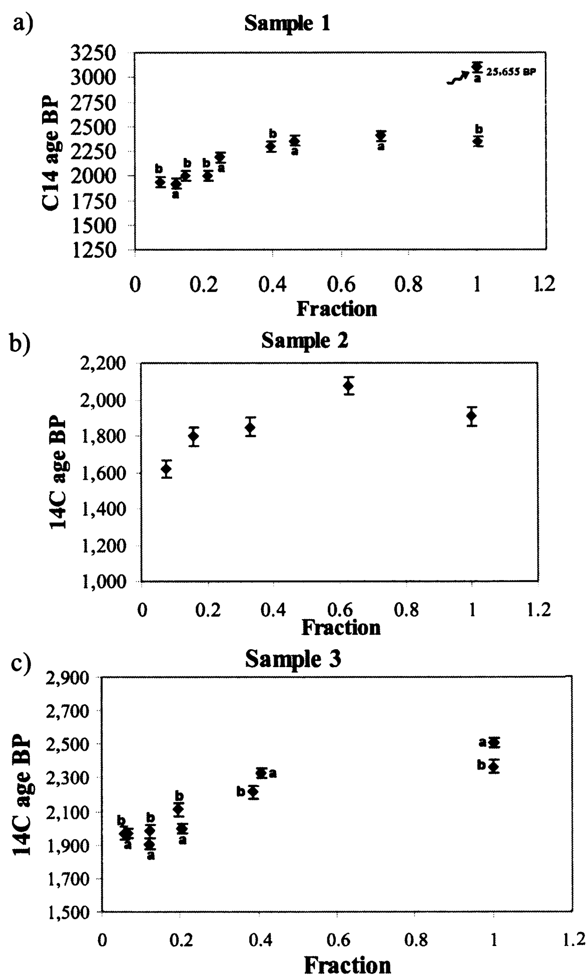

Figure 4 ^{14}C-F profiles: a) the 2 groups of determinations of sample 1 (a and b); b) sample 2; c) the 2 groups of determinations of sample 3 (a and b).

Great Temple was considered to be abandoned after the AD 363 earthquake (see X in Joukowsky 2007); however, this date contradicts that suggestion. Yet, the results agree with the interpretation of the site's excavator who underlined the impact of the earthquake on the bath complex but emphasized that reconstructions and repairs of specific spaces took place during the subsequent Byzantine Period. The bath was destroyed by another earthquake of AD 512 (during the Site's Phase XI), and subsequently abandoned, robbed and buried under accumulating sediments. In the Modern Period (phase XIV), the Bedouins used the area for farming and reused some of the architectural fragments for walls to delineate boundaries of their fields (Joukowysky 2007).

Sample 3, the water cistern at the High Place of Sacrifice: Like sample 1, 2 preparations of sample 3 were also dated. The results revealed that the initial fraction of both preparations had similar ^{14}C ages, 1961 ± 33 and 1968 ± 56 BP, respectively. Nevertheless, the second fraction of the first profile was anomalously young and had a correspondingly anomalous δ^{13}C value. The weighted average of the first 2 fractions was 1962 ± 28 ^{14}C yr BP, cal 40 BC to AD 120 at 95.4% confidence interval.

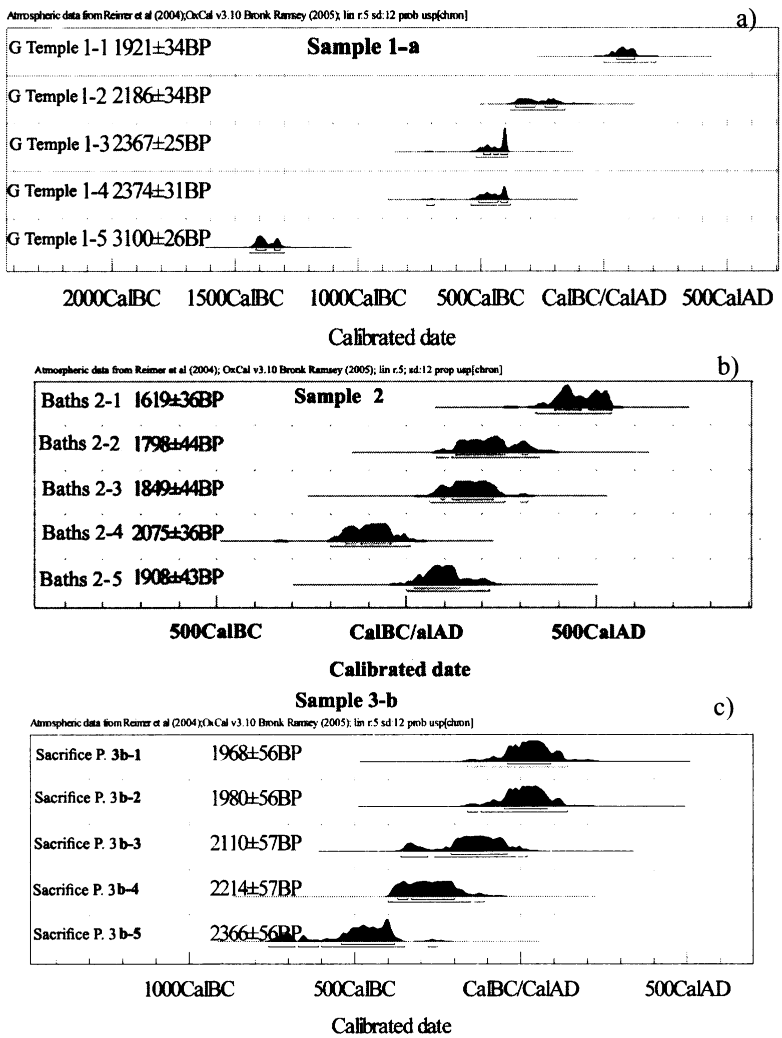

Figure 5 ^{14}C dates presented in multiple curves: a) sample 1; b) sample 2; c) sample 3

This measurement, which brackets the 1st century AD date suggested by McKenzie (1990), represents the most probable age of the plastering of the cistern and probably the carving of the sacrifice place. The remaining dates are older in age probably (as with samples 1 and 2) because of the contamination by calcareous added aggregates or under-burned limestones (Figure 5c).

CONCLUSIONS

This research presented 3 case studies of the ^{14}C dating of lime plaster samples. The results of the Great Temple samples coincide with the archaeological data, while the result of the High Place of Sacrifice sample favors the date suggested by McKenzie (1990). Modifications of the previous methods of using HCl to hydrolyze lime binder, careful collection and separation of CO_2 gas fractions, and the dolomitic limestone composition of some aggregates are possible reasons for the agreement of the results with the archaeological data. Dating the lime binder of plaster and mortar

https://doi.org/10.1017/S003382220004755X Published online by Cambridge University Press

samples from Petra provides more evidence for the potential of the applicability of the technique under careful sampling and pretreatment of the samples.

REFERENCES

Al-Bashaireh K. 2008. Chronology and technological production styles of Nabatean and Roman plasters and mortars at Petra (Jordan) [unpublished PhD dissertation]. Tucson: University of Arizona.

Al-Bashaireh K, Hodgins GWL. 2011a. AMS ^{14}C dating of organic inclusions of plaster and mortar from different structures at Petra–Jordan. *Journal of Archaeological Science* 38(3):485–91.

Al-Bashaireh K, Hodgins GWL. 2011b. AMS radiocarbon dating of lime-plaster from the Painted Room, Petra-south Jordan. In: Ringbom Å, Hohlfelder R, editors. *Proceedings from Building Roma Aeterna, conference in Rome, 23–25 March 2008*. Commentationes Humanarum Litterarum. Helsinki: Societas Scientiarium Fennica. p 231–41.

Baxter MS, Walton A. 1970. Radiocarbon dating of mortars. *Nature* 225(5236):937–8.

Bronk Ramsey C. 1995. Radiocarbon calibration and analysis of stratigraphy: the OxCal program. *Radiocarbon* 37(2):425–30.

Bronk Ramsey C. 2001. Development of the radiocarbon calibration program. *Radiocarbon* 43(2A):355–63.

Folk RL, Valastro Jr S. 1976. Successful technique for dating of lime mortar by carbon-14. *Journal of Field Archaeology* 3:203–8.

Hale J, Heinemeier J, Lancaster L, Lindroos A, Ringbom Å. 2003. Dating ancient mortar. *American Scientist* 91(2):130–7.

Heinemeier J, Jungner H, Lindroos A, Ringbom Å, von Konow T, Rud N. 1997. AMS ^{14}C dating of lime mortar. *Nuclear Instruments and Methods in Physics Research B* 123(1–4):487–95.

Heinemeier J, Ringbom Å, Lindroos A, Sveinbjörnsdóttir AE. 2010. Successful AMS ^{14}C dating of non-hydraulic lime mortars from the Medieval churches of the Åland Islands. *Radiocarbon* 52(1):171–204.

Joukowsky MS. 2002. The Petra Great Temple: a Nabataean architectural miracle. *Near Eastern Archaeology* 65(4):235–48.

Joukowsky MS. 2005. Brown University archaeological research at the Petra Great Temple, 2004. *Annual of the Department of Antiquities of Jordan* 49:147–65.

Joukowsky MS. 2007. Exciting developments: the Brown University 2006 Petra Great Temple excavations. *Annual of the Department of Antiquities of Jordan* 51:81–102.

Labeyrie J, Delibrias G. 1964. Dating of old mortars by the carbon-14 method. *Nature* 201(4920):742.

Lindroos A. 2005. Carbonate phases in historical building mortars and pozzolana concrete. Implications for AMS ^{14}C dating [unpublished PhD dissertation]. Turku: Åbo Akademi University.

Lindroos A, Heinemeier J, Ringbom Å, Braskén M, Sveinbjörnsdóttir Á. 2007. Mortar dating using AMS ^{14}C and sequential dissolution: examples from Medieval, non-hydraulic lime mortars from the Åland Islands, SW Finland. *Radiocarbon* 49(1):47–67.

McKenzie J. 1990. *The Architecture of Petra*. Oxford: Oxford University Press.

Murray MA. 1939. *Petra: The Rock City of Edom*. London: Blackie and Sons Limited.

Reimer PJ, Baillie MGL, Bard E, Bayliss A, Beck JW, Bertrand CJH, Blackwell PG, Buck CE, Burr GS, Cutler KB, Damon PE, Edwards RL, Fairbanks RG, Friedrich M, Guilderson TP, Hogg AG, Hughen KA, Kromer B, McCormac G, Manning S, Bronk Ramsey C, Reimer RW, Remmele S, Southon JR, Stuiver M, Talamo S, Taylor FW, van der Plicht J, Weyhenmeyer CE. 2004. IntCal04 terrestrial radiocarbon age calibration, 0–26 cal kyr BP. *Radiocarbon* 46(3):1029–58.

Ringbom Å, Hale J, Heinemeier J, Lindroos A, Brock F. 2006. Mortar dating in Medieval and Classical archaeology. *Constructional History Society Newsletter* 73: 11–8.

Robinson G. 1908. The High-Places of Petra. *The Biblical World* 31(1):8–21.

Sonninen E, Jungner H. 2001. An improvement in preparation of mortar for radiocarbon dating. *Radiocarbon* 43(2A):271–3.

Stuiver M, Smith CS. 1965. Radiocarbon dating of ancient mortar and plaster. In: Chatters RM, Olson EA, editors. *Proceedings of the 6th International Conference on Radiocarbon and Tritium Dating*. Washington, DC: US Department of Commerce. p 338–41.

Tubbs LE, Kinder TN. 1990. The use of AMS for the dating of lime mortars. *Nuclear Instruments and Methods in Physics Research B* 52(3–4):438–41.

Van Strydonck M, Dupas M, Dauchot-Dehon M, Pachiaudi C, Marechal J. 1986. The influence of contaminating (fossil) carbonate and the variations of δ^{13}C in mortar dating. *Radiocarbon* 28(2A):702–10.

Van Strydonck M, Dupas M, Keppens E. 1989. Isotopic fractionation of oxygen and carbon in lime mortar under natural environmental conditions. *Radiocarbon* 31(3):610–8.

Van Strydonck M, Van der Borg K, De Jong A, Keppens E. 1992. Radiocarbon dating of lime fractions and organic material from buildings. *Radiocarbon* 34(3): 873–9.

Zayadine F. 1987. Decorative stucco at Petra and other Hellenistic sites. *Studies in the History and Archaeology of Jordan* 111:131–42.